Short-time domain-wall dynamics in the random-field Ising model with a driving field

N. J. Zhou, B. Zheng,* and Y. Y. He
Zhejiang Institute of Modern Physics, Zhejiang University, Hangzhou 310027, People's Republic of China
(Received 11 May 2009; revised manuscript received 16 September 2009; published 28 October 2009)

With Monte Carlo methods, we investigate the relaxation dynamics of a domain wall in the two-dimensional random-field Ising model with a driving field. The short-time dynamic behavior at the depinning transition is carefully examined, and the roughening process of the domain wall is observed. Based on the short-time dynamic scaling form, we accurately determine the transition field, static and dynamic exponents, and local and global roughness exponents. In contrast to the usual assumption, the results indicate that the domain interface does not belong to the universality class of the Edwards-Wilkinson equation. In particular, due to the dynamic effect of overhangs, the domain interface exhibits intrinsic anomalous scaling and spatial multiscaling behaviors, compatible with the experiments.

DOI: 10.1103/PhysRevB.80.134425 PACS number(s): 64.60.Ht

I. INTRODUCTION

In recent years the dynamics of elastic systems in disordered media has been the focus of theoretical and experimental studies. Examples are charge-density waves, vortex lattices, domain walls in ferromagnetic or ferroelectric materials, contact lines, and fluid invasion in porous media.[1–5] A crucial feature of these systems is that the driven interface in disordered media displays a *depinning* phase transition at zero temperature.[6–16] In particular, the magnetic domain-wall dynamics is an important topic in magnetic devices, nanomaterials, thin films, and semiconductors.[5,17–22] The depinning transition of a *disordered* magnetic system driven by a constant field H is of second order, and its ordered parameter is the interface velocity v. If a time-dependent field $H(t)$ is applied and/or a nonzero temperature is introduced, the domain wall exhibits different states of motion and dynamic phase transitions,[19–24] and essential parts of the phenomena are also dominated by the depinning transition.

Up to date, theoretical approaches to the domain-wall dynamics in ferromagnetic and ferroelectric materials are typically based on the Edwards-Wilkinson equation with quenched disorder (QEW).[12–16,23–25] The QEW equation is a phenomenological model, and detailed microscopic structures and interactions of the materials are not concerned. The domain wall in a two-dimensional (2D) system is effectively described by a single-valued elastic string. At the depinning transition, one then expects a roughness exponent $\zeta=1$,[11,26] and this seems confirmed in numerical measurements of the *local* roughness exponent ζ_{loc} from local observables such as the height correlation function or local width function.[27,28] On the other hand, the *global* roughness exponent ζ extracted from the global width function is reported to be around 1.25 in numerical simulations.[12–14,29] Recent renormalization-group calculations up to the two-loop order also yields $\zeta=1.43$.[11] However, a roughness exponent $\zeta>1$ indicates that the elastic string is no more single-valued and one dimensional (1D).[9] This self-inconsistence is puzzling in the QEW equation. Furthermore, most experiments report $\zeta_{loc}<1$.[17,18,20]

To further understand the domain-wall motion from a more fundamental level, we should build lattice models based on microscopic structures and interactions of the materials. It may avoid the self-inconsistence, reveal new universality classes, and allow a closer comparison with experiments. The random-field Ising model with a driving field (DRFIM) is a candidate. The scaling behavior of its stationary state has been simulated at zero or low temperature, and the *static* critical exponents appear not too different from those of the QEW equation.[7,8,10,30,31] For a long time one expects that the QEW equation and DRFIM model belong to the same universality class. Due to severe *critical slowing down*, however, accurate determination of the transition field H_c and critical exponents is very difficult for the DRFIM model. Especially, the roughening dynamics of the domain wall is rarely touched, and the dynamic exponent z and roughness exponents ζ and ζ_{loc} have not been obtained. It remains a challenge whether the QEW equation and DRFIM model are really in the same universality class, especially one or both of them correctly describe the domain-wall dynamics in experiments.

In recent years much progress has been achieved in critical dynamics far from equilibrium.[32–35] Although the spatial correlation length is still short in the beginning of the time evolution, a dynamic scaling form is induced by the *divergent correlating time*. Based on the *short-time* dynamic scaling form, new methods for the determination of both dynamic and static critical exponents have been developed.[34,36] Since the measurements are carried out in the short-time regime, one does not suffer from critical slowing down. Recent activities include various applications and developments such as theoretical and numerical studies of the Josephson-junction arrays and aging phenomena.[37–44] Very recently, a kind of domain-wall roughening process at order-disorder phase transitions has been revealed.[45,46] The short-time behavior of the domain-wall relaxation at the depinning transition is also noted in simulations and experiments.[14,47] However, the short-time dynamic method has not been explored to systematically tackle the dynamic phase transitions of the domain-wall motion at zero or low temperatures such as the depinning transition and creep-relaxation transition.[20,21,23,24]

The purpose of this paper is to develop a short-time dynamic approach to the domain-wall dynamics at zero temperature, and identify the universality class of the 2D DRFIM model at the depinning transition, in comparison

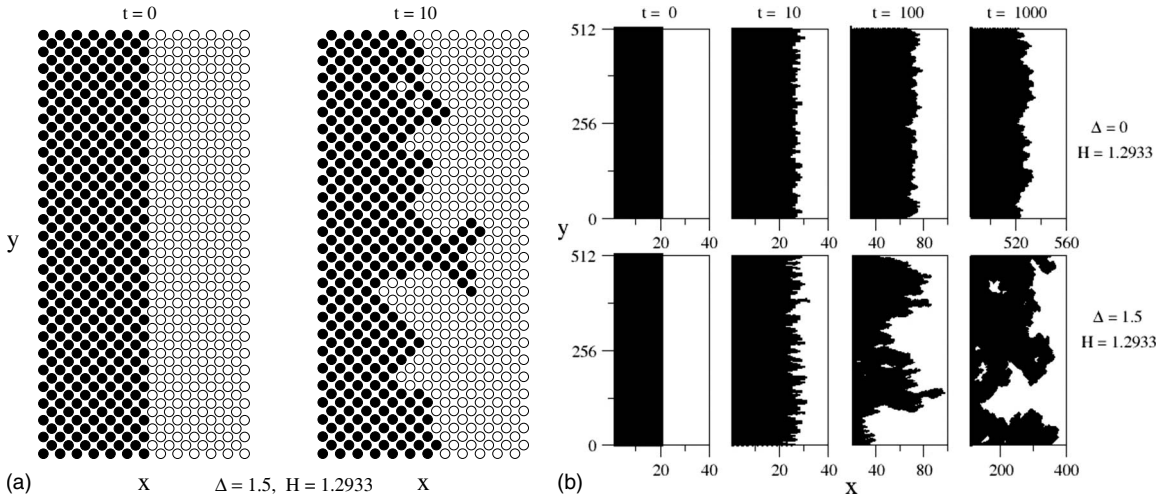

FIG. 1. (a) The initial state with a perfect domain wall, and the time evolution of the spin configuration. (b) The time evolution of the domain interface with $\Delta=0$ and $\Delta=1.5$.

with those of the QEW equation and experiments. In Sec. II, the model and scaling analysis are described, and in Sec. III, the numerical results are presented. Finally, Sec. IV includes the conclusions.

II. MODEL AND SCALING ANALYSIS

A. Model

The DRFIM model is defined by the Hamiltonian

$$\mathcal{H} = -J\sum_{\langle ij\rangle} S_i S_j - \sum_i (h_i + H)S_i. \tag{1}$$

Here $S_i = \pm 1$ is a spin at site i of a square lattice, the random field h_i is uniformly distributed within an interval $[-\Delta,\Delta]$, and H is a *homogeneous* field. Following Ref. 7, we fix $\Delta = 1.5\ J$ and set $J=1$. A Gaussian distribution of the random field h_i leads to similar results, but the fluctuations induced by the disorder are stronger and numerical simulations are technically more complicated. Therefore, we concentrate on the uniform distribution of h_i in this paper. Our simulations are performed at zero temperature with lattice sizes $L=128$, 256, 512, and 1024 up to $t_{\max}=2048$, with total samples 10,000, 40,000, 50,000 and 16,000, respectively. Main results are presented with $L=512$, and simulations of different L confirm that finite-size effects are already negligibly small. Errors are estimated by dividing the samples into two or three subgroups.

The initial state is a *semiordered* state with a perfect domain wall in the y direction. Antiperiodic and periodic boundary conditions are used in x and y directions, respectively. To eliminate the pinning effect irrelevant for disorder, we rotate the square lattice such that the initial domain wall orients in the (11) direction of the square lattice,[7,8,10] as shown in the left sector of Fig. 1(a). With the initial state, we *randomly* select a spin, and flip it if the total energy decreases after flipping. A Monte Carlo time step is defined by L^2 single-spin flips. As time evolves, the domain wall moves and roughens while the bulk remains unchanged. Therefore, we call it *a domain interface*. We should emphasize that for $\Delta \geq 1$, *overhangs* and *islands* will be created, but only by the domain wall. It still makes sense to define the interface. In Fig. 1(b), the time evolution of the spin configurations is displayed for $\Delta=0$ and $\Delta \geq 1$. The fine structure of the spin configuration of $\Delta \geq 1$ is shown in the right sector of Fig. 1(a). For a fixed $\Delta \geq 1$ and at the depinning transition field H_c, the interface width continuously increases with time and finally diverges if the lattice size is infinite. This is a kind of roughening transition. For $\Delta=0$, the domain interface also grows continuously, but it belongs to the universality class of $H \gg H_c$.[13,14]

Due to the existence of the overhangs and islands, there may be different ways to define the domain interface. We adopt the one commonly used in the literature.[7,10] Denoting a spin at site (x,y) by $S_{xy}(t)$, we first introduce a height function

$$h(y,t) = \frac{1}{L}\sum_x S_{xy}(t), \tag{2}$$

and then define the line magnetization $h(t) \equiv h^{(1)}(t)$ and its second moment $h^{(2)}(t)$,

$$h^{(k)}(t) = \langle [h(y,t)]^k \rangle, \quad k = 1,2, \tag{3}$$

where $\langle \cdots \rangle$ includes the statistical average and average over y. In the height function $h(y,t)$ defined in Eq. (2), the contribution of overhangs and islands seems formally suppressed. However, overhangs and islands essentially affect the dynamic evolution of the spin configuration and do play essential roles in the interface movement and growth. With the height function at hand, the average velocity of the interface can be calculated as[7]

$$v(t) = \frac{L}{2}\frac{dh(t)}{dt}. \tag{4}$$

Here $v(t)$ is the order parameter of the depinning phase transition. On the other hand, the domain interface itself is rep-

resented by the height function $h(y,t)$. Therefore, the roughness function of the interface is defined as

$$\omega^2(t) = h^{(2)}(t) - h(t)^2. \tag{5}$$

A more informative quantity is the height correlation function

$$C(r,t) = \langle [h(y+r,t) - h(y,t)]^2 \rangle, \tag{6}$$

which describes both the spatial correlation of the height function and the growth of the interface. To obtain the dynamic exponent z *independently*, we introduce an observable

$$F(t) = [M^{(2)}(t) - M(t)^2]/\omega^2(t). \tag{7}$$

Here $M(t)$ is the global magnetization and $M^{(2)}(t)$ is its second moment. In fact, $F(t)$ is nothing but the ratio of the planar susceptibility and line susceptibility.

B. Scaling analysis

Since the depinning transition is a second-order phase transition, the dynamic evolution of the order parameter $v(t)$ should obey the dynamic scaling theory supported by the renormalization-group calculations.[32,34,36] For a finite lattice size L, and assuming a nonequilibrium correlation length $\xi(t) \sim t^{1/z}$, scaling arguments lead to a dynamic scaling form of the order parameter,[32,34,36]

$$v(t,\tau,L) = b^{-\beta/\nu} v(b^{-z}t, b^{1/\nu}\tau, b^{-1}L). \tag{8}$$

Here b is an arbitrary rescaling factor, β and ν are the static exponents, z is the dynamic exponent, and $\tau = (H - H_c)/H_c$. Taking $b \sim \xi(t) \sim t^{1/z}$, the dynamic scaling form can be rewritten as

$$v(t,\tau,L) = t^{-\beta/\nu z} v(1, t^{1/\nu z}\tau, t^{-1/z}L). \tag{9}$$

In the short-time regime, i.e., the regime with $\xi(t) \sim t^{1/z} \ll L$, the finite-size effect is negligibly small. Therefore,

$$v(t,\tau) = t^{-\beta/\nu z} G(t^{1/\nu z}\tau). \tag{10}$$

At the depinning transition point $\tau = 0$, the scaling form leads to a power law

$$v(t) \sim t^{-\beta/\nu z}. \tag{11}$$

With Eq. (10), one may locate the critical field H_c by searching for the best power-law behavior of $v(t,\tau)$.[34,36] To determine ν, one simply derives from Eq. (10)

$$\partial_\tau \ln v(t,\tau)|_{\tau=0} \sim t^{1/\nu z}. \tag{12}$$

In general, even at the transition point $\tau = 0$, $\omega^2(t)$ and $C(r,t)$ do not obey a simple power-law behavior, for the order parameter is $v(t)$, *not* $h(t)$. In fact, the interface also roughens even *without* disorder. This leads to rather strong corrections to scaling. To capture the dynamic effects of disorder, we introduce the pure roughness function

$$D\omega^2(t) = \omega^2(t) - \omega_b^2(t), \tag{13}$$

and height correlation function

$$DC(r,t) = C(r,t) - C_b(r,t), \tag{14}$$

where $\omega_b^2(t)$ and $C_b(r,t)$ are the roughness function and height correlation function for $\Delta = 0$. For a sufficiently large lattice and at the transition point $\tau = 0$, $D\omega^2(t)$ and $DC(r,t)$ should then obey the standard power-law scaling forms[6,27,29]

$$D\omega^2(t) \sim t^{2\zeta/z} \tag{15}$$

and

$$DC(r,t) \sim \begin{cases} t^{2(\zeta-\zeta_{loc})/z} r^{2\zeta_{loc}} & \text{if } r \ll \xi(t) \ll L \\ t^{2\zeta/z} & \text{if } 0 \ll \xi(t) \ll r \end{cases}. \tag{16}$$

Here $\xi(t) \sim t^{1/z}$, ζ is the global roughness exponent, and ζ_{loc} is the local one. In Refs. 45 and 46, the finite-size scaling behavior of $D\omega^2(t)$ has been carefully analyzed and it reveals

$$D\omega^2(t) \sim L^{-2}. \tag{17}$$

In the short-time regime, the spatial correlation length of $h(y,t)$ is small. Therefore, the finite-size dependence of $DC(r,t)$ is the same as that of $D\omega^2(t)$,

$$DC(r,t) \sim L^{-2}. \tag{18}$$

Since $\omega^2(t)$ describes the fluctuation in the x direction and $M^{(2)}(t) - M(t)^2$ includes those in both the x and y directions, the dynamic scaling behavior of $F(t)$ is[34,45]

$$F(t) \sim \xi(t)/L \sim t^{1/z}/L. \tag{19}$$

Here we need not redefine $F(t)$ with $D\omega^2(t)$, for the correction to scaling induced by $\omega_b^2(t)$ cancels with that in $M^{(2)}(t) - M(t)^2$.

III. NUMERICAL RESULTS

In Fig. 2(a), the interface velocity $v(t,\tau)$ is displayed for different driving field H with $L = 512$. The velocity drops rapidly down for smaller H, while approaches a constant for larger H. Searching for the best power-law behavior, one locates the transition field $H_c = 1.2933(2)$. This value is much more precise than $H_c = 1.290(3)$ obtained from the steady state.[7] In Fig. 2(a), one observes that $v(t,\tau)$ at $H_c = 1.2933(2)$ shows an almost-perfect power-law behavior starting from rather early times and in about three orders of magnitude. According to Eq. (11), one measures the exponent $\beta/\nu z = 0.217(2)$ from the slope of the curve at H_c. In Fig. 2(b), the dynamic observable $F(t)$ defined in Eq. (7) is plotted at $H = H_c = 1.2933$. A nice power-law behavior is detected for both $\Delta = 1.5$ and $\Delta = 0$. Based on Eq. (19), $1/z = 0.749(5)$ and $1/z_b = 0.666(4)$ are derived from the slopes of the curves at $H = 1.2933$ for $\Delta = 1.5$ and 0, respectively.

To investigate the possible finite-size effects, $v(t)$ and $F(t)$ computed with different lattice sizes at $H_c = 1.2933(2)$ are also plotted in Fig. 2. The finite-size scaling analysis in Eq. (9) shows that at the critical point $v(t) \sim t^{-\beta/\nu z} f(t/L^z)$. In the short-time regime, however, the finite-size effect described by $f(t/L^z)$ can be easily controlled, i.e., it rapidly disappears as L increases. This is a merit of the short-time dynamic approach.[34–36,45,46] Similarly, one may deduce $F(t) \sim t^{1/z} g(t/L^z)/L$.[34,45] To verify the finite-size dependence of

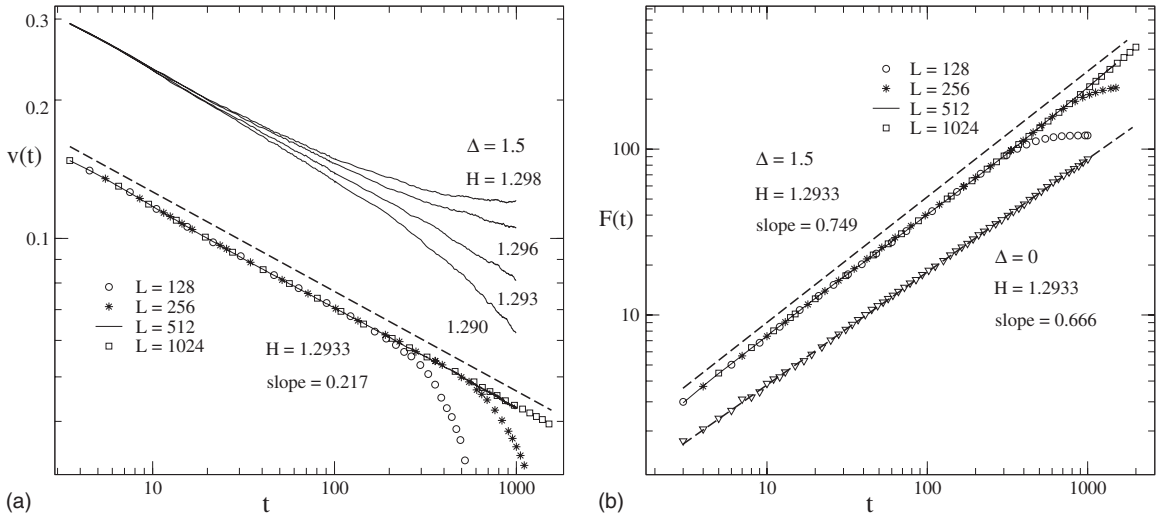

FIG. 2. (a) Interface velocity $v(t,\tau)$ is displayed for different driving fields H on a log-log scale. For clarity, the curves at $H_c=1.2933$ with different lattice sizes are shifted down. (b) $F(t)$ is plotted for $\Delta=1.5$ and 0 at $H_c=1.2933$. To reveal the finite-size dependence in Eq. (19), $F(t)$ has been rescaled by a factor L. In both (a) and (b), dashed lines show power-law fits.

$F(t)$, $F(t)$ is actually rescaled by a factor L in Fig. 2(b), i.e., the y axis is $F(t)L$. The finite-size effect described by $g(t/L^z)$ also drops down rapidly. In Fig. 2, one clearly observes that the curves of $L=512$ and 1048 overlap at least up to $t=1000$. We measure $\beta/\nu z=0.215(2)$ and $1/z=0.745(9)$ from the curves of $L=1048$, in good agreement with those from $L=512$ within errors.

To calculate the logarithmic derivative $\partial_\tau \ln v(t,\tau)=\partial_\tau v(t,\tau)/v(t,\tau)$, we quadratically interpolate $v(t,\tau)$ between $H=1.290$ and 1.298 with the data in Fig. 2(a). In Fig. 3(a), $\partial_\tau \ln v(t,\tau)$ is plotted at $H_c=1.2933$. A power-law behavior is observed but with certain corrections to scaling at the early times. According to Eq. (12), a direct measurement from the slope of the curve gives $1/\nu z=0.729$. After introducing a power-law correction to scaling to Eq. (12), i.e., $\partial_\tau \ln v(t)\sim t^{1/\nu z}(1+c/t)$, the fitting to the numerical data extends to early times, and it yields $1/\nu z=0.735(10)$.

In Fig. 3(b), the roughness functions $\omega^2(t)$ and $\omega_b^2(t)$ for $\Delta=1.5$ and 0 at $H=1.2933$, and the pure roughness function $D\omega^2(t)=\omega^2(t)-\omega_b^2(t)$ are displayed with $L=512$. The curve $\omega^2(t)$ with $L=1024$ is also plotted for comparison. To reveal the finite-size dependence, the y axis has been rescaled by a factor L^2. Obviously $D\omega^2(t)$ shows a cleaner power-law behavior than $\omega^2(t)$ does, due to the subtraction of $\omega_b^2(t)$. The slope of the curve $D\omega^2(t)$ is 1.701(6). To further refine this result, we consider a power-law correction to Eq. (16), i.e., $D\omega^2(t)\sim t^{2\zeta/z}(1+c/t)$, and it leads to $2\zeta/z=1.717(7)$. In a similar way we derive $2\zeta_b/z_b=0.649(4)$ from $\omega_b^2(t)$.

In Fig. 4(a), the pure height correlation function $DC(r,t)$ is displayed for $\Delta=1.5$ at H_c. For a large $r\gg\xi(t)$, e.g., $r=256$, one extracts the exponent $2\zeta/z=1.701(8)$ by Eq. (16), consistent with that from Fig. 3(b). For a small $r\ll\xi(t)$,

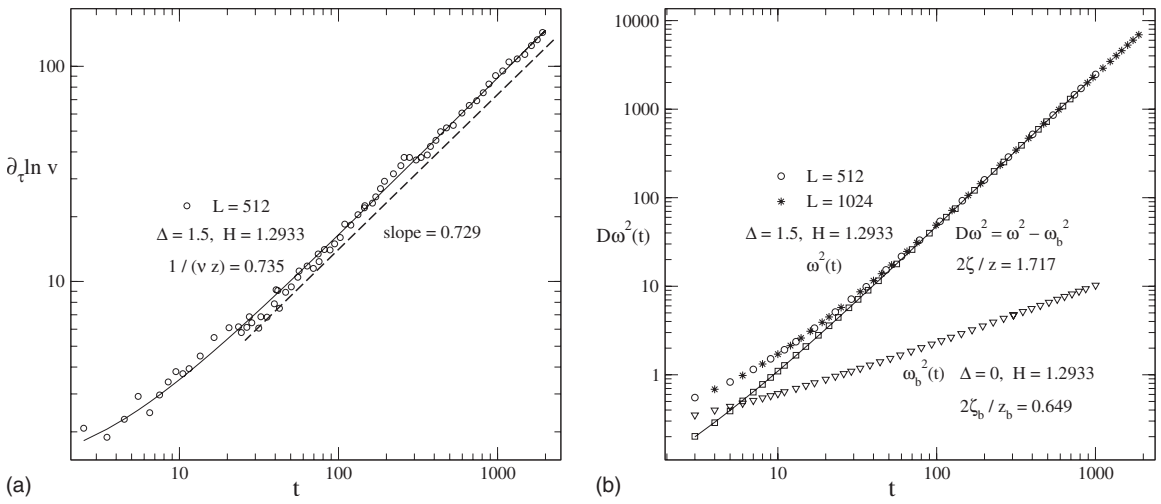

FIG. 3. (a) The logarithmic derivative of $v(t,\tau)$ is displayed for $\Delta=1.5$ at $H_c=1.2933$. The dashed line represents a power-law fit. (b) Roughness functions $\omega^2(t)$ and $\omega_b^2(t)$ for $\Delta=1.5$ and 0 at $H_c=1.2933$ are plotted. Squares represent the pure roughness function $D\omega^2(t)$. To show the finite-size dependence in Eq. (17), the y axis has been rescaled by a factor L^2. In both (a) and (b), solid lines show power-law fits with corrections and the corrections refine the exponents by about one percent.

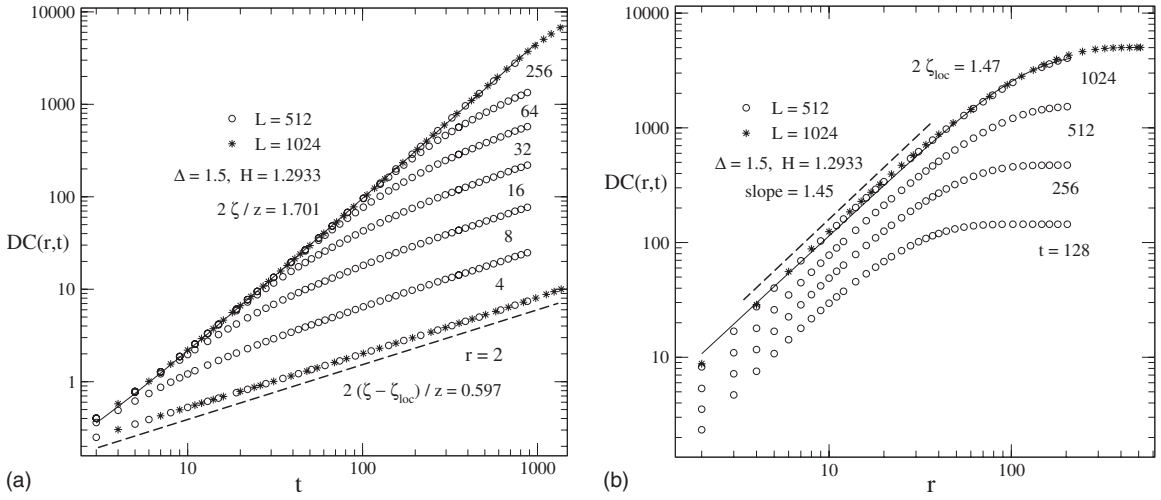

FIG. 4. (a) The time evolution of the pure height correlation function $DC(r,t)$ is displayed for different r. (b) $DC(r,t)$ is plotted as a function of r at different t. In both (a) and (b), dashed lines represent power-law fits and solid lines show power-law fits with corrections. To reveal the finite-size dependence in Eq. (18), $DC(r,t)$ has been rescaled by a factor L^2.

$DC(r,t)$ should be independent of t for a normal interface with $\zeta=\zeta_{loc}$, according to Eq. (16). But $DC(r,t)$ of $r=2$ in Fig. 4(a) clearly increases with t. A perfect power-law behavior is observed with an exponent $2(\zeta-\zeta_{loc})/z=0.597(4)$. Without subtracting $C_b(r,t)$, one needs simulations up to longer times to expose the scaling behavior of $C(r,t)$. Finally, some curves of $L=1048$ are also shown in Fig. 4(a). The resulting exponents are the same as those from $L=512$ within errors. To confirm the finite-size behavior in Eq. (18), $DC(r,t)$ is actually rescaled by a factor L^2 in Fig. 4(a).

From the measurements of $\beta/\nu z$, $1/\nu z$, $1/z$, $2\zeta/z$, and $2(\zeta-\zeta_{loc})/z$, we calculate the critical exponents $\beta=0.295(3)$, $\nu=1.02(2)$, $z=1.33(1)$, $\zeta=1.14(1)$, and $\zeta_{loc}=0.735(8)$ for the depinning transition. The local roughness exponent $\zeta_{loc}=0.735(8)$ can be further confirmed by the scaling behavior $DC(r,t)\sim r^{2\zeta_{loc}}$ for $r\ll\xi(t)$ in Eq. (16), but this regime is narrow. In Fig. 4(b), $DC(r,t)$ is plotted as a function of r. In the regime $4\leq r\leq 40$, one indeed obtains $\zeta_{loc}=0.725$ from the slope of the curve. For larger r, however, there emerge strong corrections to scaling. An extended scaling form could lead to a better fitting to the numerical data and yields $\zeta_{loc}=0.735(15)$.[6,27]

All the measurements of the critical exponents are summarized in Table I, in comparison with those in the literature and for the QEW equation. Our transition field H_c and static exponents β and ν of the DRFIM model significantly refine those in the literature.[7,30,31] For the first time, we obtain the dynamic exponent z and roughness exponents ζ and ζ_{loc}. For the QEW equation and its variants, there have been various measurements of the critical exponents. We list only those in the recent decade and clearly for the QEW equation. In Ref. 9, for example, it is reported $\zeta\approx 1.17$, but a nonlocal Monte Carlo algorithm has been applied. Other examples are $\zeta=1.15$ for a self-organized growth model[49] and for a discrete string.[50] These variants might not be in the universality class of the QEW equation. For the QEW equation, theoretically one may expect $\zeta_{loc}=1$, but numerically it is difficult to extract it from $DC(r,t)\sim r^{2\zeta_{loc}}$ in Eq. (16), and one should consider corrections to scaling.[6,27] In Ref. 28, the correction to scaling has not been taken into account, thus $\zeta_{loc}=0.92$ is smaller. Our analysis in this paper shows that it is more accurate to measure ζ_{loc} from $DC(r,t)\sim t^{2(\zeta-\zeta_{loc})/z}$ in Eq. (16). After a careful survey of the literature, we believe that real

TABLE I. The depinning transition field and critical exponents obtained with the short-time dynamic approach are compared with those in the literature and for the QEW equation. The lower sector is for the DRFIM model with $\Delta=0$ and QEW equation with $H\gg H_c$. All results are from numerical simulations.

		QEW	DRFIM	This work
$v(t)$	H_c		1.290(3) (Ref. 7)	1.2933(2)
	β	0.33(2) (Ref. 13); 0.33 (Ref. 14)	0.35(4) (Ref. 7); 0.31(8) (Ref. 30)	0.295(3)
	ν	1.29(5) (Ref. 13); 1.33 (Ref. 14); 1.33(1) (Ref. 48)	1.00(5) (Ref. 7); 1.33 (Ref. 31)	1.02(2)
	z	1.5 (Ref. 14); 1.53 (Ref. 28)		1.33(1)
$\omega^2(t)$	ζ	1.26(1) (Refs. 12, 13, and 15); 1.25 (Ref. 14); 1.24 (Ref. 28)		1.14(1)
$C(r,t)$	ζ	1.23(1) (Ref. 29); 1.25 (Ref. 28)		1.13(1)
	ζ_{loc}	0.98 (Ref. 27); 0.92 (Ref. 28)		0.735(8)
$H\gg H_c$	z_b	1.5 (Ref. 14)		1.50(1)
	ζ_b	0.5 (Ref. 13)		0.49(1)

critical exponents of the QEW equation should be close to those summarized in Table I.

Finally we should mention that the depinning transition could be relevant for the percolation of the geometric clusters in the 2D DRFIM model.[51,52] Deeper understanding of this kind, however, needs further investigations.

IV. CONCLUSIONS

To summarize, we have developed a short-time dynamic approach to the domain-wall dynamics of the DRFIM model at the depinning transition. The method does not suffer from critical slowing down, and it can be generally applied to different dynamic phase transitions of the domain-wall motion. With our accurate measurements of all critical exponents, we are now able to compare the DRFIM model with the QEW equation. First, the exponents β, z, and ζ of the DRFIM model differ from those of the QEW equation by about 10 percent, and especially the difference in ν and ζ_{loc} between two models reaches nearly 30 percent. These deviations could not be ruled out by statistical errors. Second, the DRFIM model belongs to a universality class with intrinsic anomalous scaling and spatial multiscaling, i.e., $\zeta > 1$ and $\zeta_{loc} < 1$, while the QEW equation is with super-rough scaling and spatial single scaling, i.e., $\zeta > 1$ and $\zeta_{loc} = 1$.[27,29,53] These results indicate that the DRFIM model and QEW equation are not in a same universality class.

In the DRFIM model, overhangs and islands naturally develop, thus the domain wall is not single-valued and one dimensional. Therefore, there exists no self-inconsistence. In the QEW equation, even if overhangs and islands might be created in peculiar ways, the growth dynamics should be different from that of the DRFIM model. To show the importance of overhangs and islands, we perform simulations of the DRFIM model with $\Delta = 0$ at $H = 1.2933$. As shown in Table I, the exponents z_b and ζ_b are the same as those of the QEW equation with $H \gg H_c$, since overhangs and islands are suppressed in both models.

Experimental measurements of the roughness exponents of the domain interface at zero temperature do not exist. For $T > 0$ and $0 < H < H_c$, it is reported that $\zeta_{loc} = 0.7(1)$ and 0.69(7) in the experiments with ultrathin Pt/Co/Pt films,[17,20] and $\zeta_{loc} = 0.78(1)$ with $Co_{28}Pt_{72}$ alloy films.[18] Our numerical value $\zeta_{loc} = 0.735(8)$ is compatible with these experimental results.

ACKNOWLEDGMENTS

This work was supported in part by National Natural Science Foundation of China under Grant Nos. 10875102 and 10325520, and Natural Science Foundation of Zhejiang Province of China under Grant No. Z6090130.

*Corresponding author; zheng@zimp.zju.edu.cn

[1] S. Brazovskii and T. Nattermann, Adv. Phys. **53**, 177 (2004).
[2] P. Paruch, T. Giamarchi, and J. M. Triscone, Phys. Rev. Lett. **94**, 197601 (2005).
[3] P. Le Doussal, K. J. Wiese, E. Raphael, and R. Golestanian, Phys. Rev. Lett. **96**, 015702 (2006).
[4] M. Rost, L. Laurson, M. Dube, and M. Alava, Phys. Rev. Lett. **98**, 054502 (2007).
[5] M. Yamanouchi, J. Ieda, F. Matsukura, S. E. Barnes, S. Maekawa, and H. Ohno, Science **317**, 1726 (2007).
[6] M. Jost and K. D. Usadel, Phys. Rev. B **54**, 9314 (1996).
[7] U. Nowak and K. D. Usadel, Europhys. Lett. **44**, 634 (1998).
[8] L. Roters, A. Hucht, S. Lübeck, U. Nowak, and K. D. Usadel, Phys. Rev. E **60**, 5202 (1999).
[9] A. Rosso and W. Krauth, Phys. Rev. Lett. **87**, 187002 (2001).
[10] L. Roters, S. Lübeck, and K. D. Usadel, Phys. Rev. E **63**, 026113 (2001).
[11] P. Le Doussal, K. J. Wiese, and P. Chauve, Phys. Rev. B **66**, 174201 (2002).
[12] A. Rosso, A. K. Hartmann, and W. Krauth, Phys. Rev. E **67**, 021602 (2003).
[13] O. Duemmer and W. Krauth, Phys. Rev. E **71**, 061601 (2005).
[14] A. B. Kolton, A. Rosso, E. V. Albano, and T. Giamarchi, Phys. Rev. B **74**, 140201(R) (2006).
[15] A. B. Kolton, A. Rosso, T. Giamarchi, and W. Krauth, Phys. Rev. Lett. **97**, 057001 (2006).
[16] S. Bustingorry, A. B. Kolton, and T. Giamarchi, Europhys. Lett. **81**, 26005 (2008).
[17] S. Lemerle, J. Ferré, C. Chappert, V. Mathet, T. Giamarchi, and P. Le Doussal, Phys. Rev. Lett. **80**, 849 (1998).
[18] M. Jost, J. Heimel, and T. Kleinefeld, Phys. Rev. B **57**, 5316 (1998).
[19] T. Braun, W. Kleemann, J. Dec, and P. A. Thomas, Phys. Rev. Lett. **94**, 117601 (2005).
[20] P. J. Metaxas, J. P. Jamet, A. Mougin, M. Cormier, J. Ferre, V. Baltz, B. Rodmacq, B. Dieny, and R. L. Stamps, Phys. Rev. Lett. **99**, 217208 (2007).
[21] W. Kleemann, J. Rhensius, O. Petracic, J. Ferré, J. P. Jamet, and H. Bernas, Phys. Rev. Lett. **99**, 097203 (2007).
[22] A. Dourlat, V. Jeudy, A. Lemaître, and C. Gourdon, Phys. Rev. B **78**, 161303(R) (2008).
[23] T. Nattermann, V. Pokrovsky, and V. M. Vinokur, Phys. Rev. Lett. **87**, 197005 (2001).
[24] A. Glatz, T. Nattermann, and V. Pokrovsky, Phys. Rev. Lett. **90**, 047201 (2003).
[25] W. Kleemann, Annu. Rev. Mater. Res. **37**, 415 (2007).
[26] T. Nattermann, S. Stepanow, L. H. Tang, and H. Leschhorn, J. Phys. II France **2**, 1483 (1992).
[27] M. Jost and K. D. Usadel, in *Chaos and Fractals in Chemical Engineering*, edited by G. Biardi, M. Giona, and A. R. Giona (World Scientific, Singapore, 1997).
[28] J. M. López and M. A. Rodríguez, J. Phys. I **7**, 1191 (1997).
[29] N. N. Pang and W. J. Tzeng, Phys. Rev. E **61**, 3212 (2000).
[30] Luís A. Nunes Amaral, A. L. Barabási, and H. E. Stanley, Phys. Rev. Lett. **73**, 62 (1994).
[31] C. S. Nolle, B. Koiller, N. Martys, and M. O. Robbins, Physica A **205**, 342 (1994).
[32] H. K. Janssen, B. Schaub, and B. Schmittmann, Z. Phys B **73**,

539 (1989).
[33] D. A. Huse, Phys. Rev. B **40**, 304 (1989).
[34] B. Zheng, Int. J. Mod. Phys. B **12**, 1419 (1998).
[35] B. Zheng, M. Schulz, and S. Trimper, Phys. Rev. Lett. **82**, 1891 (1999).
[36] H. J. Luo, L. Schülke, and B. Zheng, Phys. Rev. Lett. **81**, 180 (1998).
[37] Y. Ozeki and N. Ito, Phys. Rev. B **68**, 054414 (2003).
[38] E. Granato and D. Dominguez, Phys. Rev. B **71**, 094521 (2005).
[39] P. Calabrese and A. Gambassi, J. Phys. A **38**, R133 (2005).
[40] X. W. Lei and B. Zheng, Phys. Rev. E **75**, 040104(R) (2007).
[41] S. Z. Lin and B. Zheng, Phys. Rev. E **78**, 011127 (2008).
[42] E. V. Albano and G. Saracco, Phys. Rev. Lett. **88**, 145701 (2002).
[43] M. Pleimling and F. Iglói, Phys. Rev. Lett. **92**, 145701 (2004).
[44] H. K. Lee and Y. Okabe, Phys. Rev. E **71**, 015102(R) (2005).
[45] N. J. Zhou and B. Zheng, Phys. Rev. E **77**, 051104 (2008).
[46] Y. Y. He, B. Zheng, and N. J. Zhou, Phys. Rev. E **79**, 021107 (2009).
[47] G. Rodríguez-Rodríguez, A. Pérez-Junquera, M. Vélez, J. V. Anguita, J. I. Martín, H. Rubio, and J. M. Alameda, J. Phys. D **40**, 3051 (2007).
[48] C. J. Bolech and A. Rosso, Phys. Rev. Lett. **93**, 125701 (2004).
[49] K. Park and I. M. Kim, Phys. Rev. E **59**, 5150 (1999).
[50] H. J. Jensen, J. Phys. A **28**, 1861 (1995).
[51] E. T. Seppälä and M. J. Alava, Phys. Rev. E **63**, 066109 (2001).
[52] L. Környei and F. Iglói, Phys. Rev. E **75**, 011131 (2007).
[53] M. Pradas, A. Hernandez-Machado, and M. A. Rodríguez, Phys. Rev. E **77**, 056305 (2008).